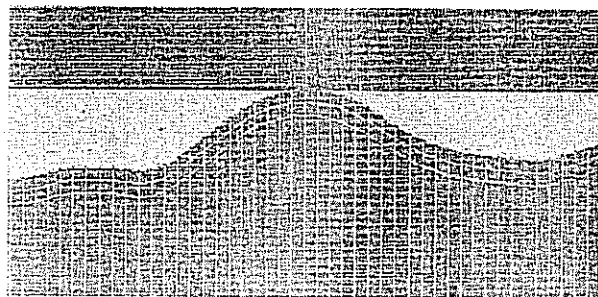
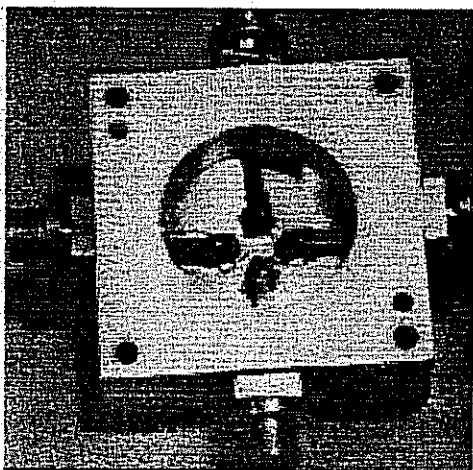
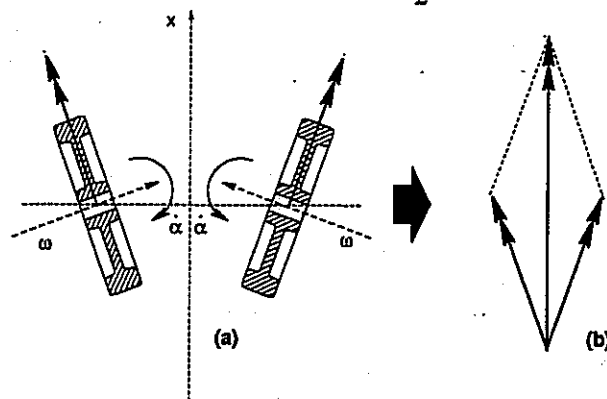
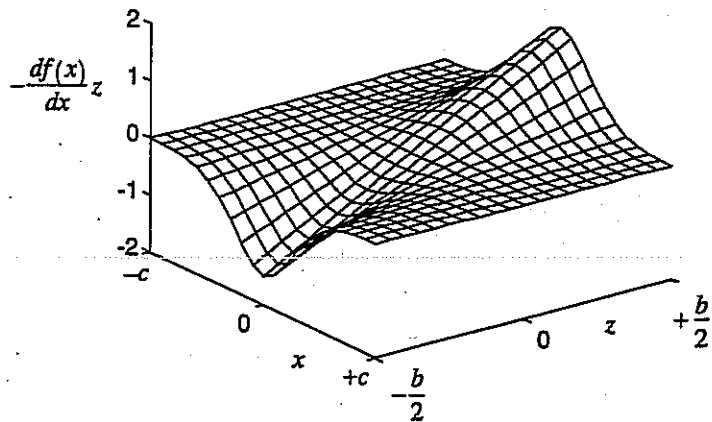
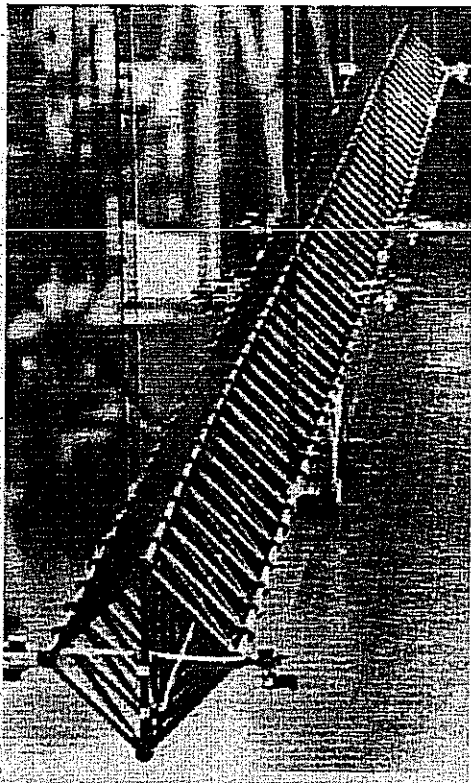


International Journal of Mechanics and Control

Editor in Chief: Ario Romiti
Managing editor: Andrea Manuello Bertetto



CONTENTS

- 3 **Adaptive Control of a Large Space Structure using Lattice Filters**
F. Bernelli-Zazzera, L. Dozio, P. Mantegazza
- 19 **Closed form solution for non tubular bonded joints with tapered adherends under torsion**
N. Pugno
- 29 **On the Gyroscopic Stabilisation of a Single Track Vehicle: Free Control Response in Straight Ahead Driving**
A. Baldi
- 41 **Assessment of Real Contact Area in wheel-rail interfaces: comparison between ultrasonic technique and FEM analysis**
M. Pau, M. Ruggiu
- 49 **A novel pneumatic valve actuated by Shape Memory Alloy wires**
C. Ferraresi, D. Maffiodo, A. Manuello Bertetto

next number scheduled titles:

Mechanical Transmissions for Electrical and Diesel-Electrical Locomotives
G. Roccati and D. Botto

On the Gyroscopic Stabilisation of a Single Track Vehicle: Experimental Results
A. Baldi

High Deformation Strain Gauge for non Conventional Robotics
W. Franco, D. Maffiodo, A. Manuello Bertetto

Electrical flight controls feasibility study for aircraft models
P. Maggiore

Geometrical parameters influence on the performances of a pneumatic low friction seal
G. Belforte, A. Manuello Bertetto, L. Mazza

Closed form solution for non tubular bonded joints with tapered adherends under torsion

Nicola Pugno

Department of Structural Engineering
Politecnico di Torino

Keywords: bonded joint, non-tubular, tapered adherends, torsion.

Abstract

The object of the present paper is the study of an adhesive bonded non tubular joint with tapered adherends subjected to torsion. The joint considered consists of two rectangular section beams bonded together along a side surface.

The work emphasized how the stress field developed in the adhesive at the bond area between the two beams is heavily dependent on joint geometry: the maximum stresses for a joint without tapered adherends are reached at the ends of the adhesive while they appear along its centerline if the adherends are tapered.

The analytical equations which govern torsional moment section by section in the joint, stresses and strains in the adhesive and the joint's elastic strain (rotation between the two beams) are obtained as power series with coefficients given in closed recursive form.

1 Introduction

As the literature indicates, studies on adhesive bonded joints have hitherto concentrated on the effects of tension or compression, flexure and shear. In certain situations, however, such joints are also subject to torsion. Research in this area is restricted to tubular structures, and only recently non-tubular bonded joints have been studied. [15-18].

Since the two pioneer papers of Goland and Reissner [7] and Lubkin and Reissner [12] tubular joints subject to torsion have been studied from many different points of view.

Theoretical approaches have been validated experimentally and numerically; Fracture Mechanics has been used to solve the problem of the joint's strength in the case of brittle collapse with static or fatigue loading; the non-linear and viscoelastic adhesive's behaviour has been considered and recently also the dynamic analysis have been carried out. Specifically in the works of Hipol [9] and Chen and Cheng [5] it is emphasized the positive influence of tapering at the adherends' end on the stress peaks in the adhesive layer respectively from a numerical and a theoretical point of view: if the adherends are partially-tapered the stress peaks become lower.

The lack of work on non-tubular joints indicated by this bibliography motivated the investigation presented in the work developed by Pugno [16] and Pugno, Surace [17]. Pugno and Surace [17] have studied a non tubular joint subjected to torsion from a theoretical point of view validated numerically by a three dimensional finite element analysis.

Contact author: Nicola Pugno

Department of Structural Engineering,
Politecnico di Torino,
Corso Duca degli Abruzzi 24,
10129 Torino, Italy.
Tel: +39.115644895; Fax: +39.115644899;
E-mail: pugno@polito.it

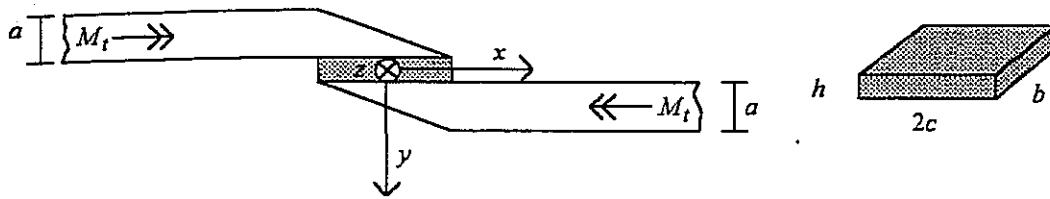


Fig. 1 Rectangular tapered adherends in a non-tubular bonded joint under torsion

In Pugno's paper [16] the non tubular joint is optimized for uniform torsional strength: starting from a non tapered joint the optimization was achieved by chamfering the edges, which are in any case not involved in the stress flow induced by the tensile loading for which the joint should be designed. The resulting optimized joint is thus both lighter and stronger. The same results for tubular joints is presented in the work of Pugno and Surace [18], where the joint is optimized for uniform torsional strength.

The present paper wants to extend to the study of a non tubular joint subjected to torsion in the case of tapered adherends.

2 Mathematical model

It is assumed that the materials making up the joint (Figure 1) are governed by a linear elastic law (in particular the materials are assumed isotropic). While this is intuitively obvious for the beams (which are typically metal), this is not the case for the adhesive, which is more likely to show a typically non-linear elastic behaviour.

Under torsion, however, the stress state in the adhesive relative to a non-tubular bonded joint is basically normal. As it is well known that adhesive can withstand tangential stresses which are an order of magnitude higher than the ultimate normal stresses, it follows that the normal stresses occurring in the adhesive during service must be limited. It is precisely because of these modest stresses that we can assume that the adhesive is also governed by a linear elastic law and that it is verify also the

geometrical linearity. The adherends can be studied with the Technical Theory of Beams. Assuming linear elastic laws and using equilibrium and compatibility equations to solve the torsional problem [16,17], the function which governs transmission of the torsional moment along the overlap, or in other words, how the torsional moment progresses section by section along the top beam, can be found by solving the following differential equation:

$$\frac{d^2 M(x)}{dx^2} + \frac{K^* I_1(x) + I_2(x)}{G I_1(x) I_2(x)} M(x) = \frac{K^* M_t}{G I_1(x)} \begin{cases} M(x = -c) = M_t \\ M(x = c) = 0 \end{cases} \quad (1)$$

where x is the longitudinal coordinate of the joint (Figure 1).

The torsional moment on the top beam found section by section in the thin adhesive layer is designated as M , while K^* is the adhesive specific (per unit length) stiffness, G is the shear elastic modulus of the two beams and I_i is their factor of torsional rigidity.

The adhesive specific stiffness can be expressed as:

$$K^* = \frac{(1-\nu_a)E_a}{(1+\nu_a)(1-2\nu_a)} \frac{b^3}{12h} = E_a^* \frac{I_x^*}{h} \quad (2)$$

where ν_a, E_a are the Poisson's ratio and Young's modulus respectively of the adhesive, h is its thickness, b is the base of the beam's cross section (Figure 1), while $I_x^* = b^3/12, E_a^*$ indicate respectively a specific moment of inertia and the adhesive's fictitious Young modulus.

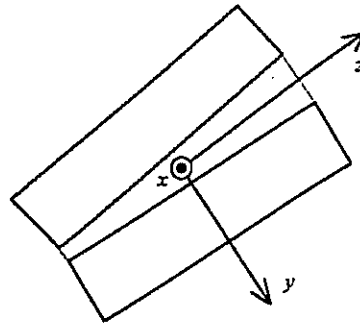


Fig. 2 Predominant elastic strain ϵ_y in a joint's cross section due to the relative rotation between the two beams

In the case of rectangular tapered section here considered, the factor of torsional rigidity can be expressed by the following equation:

$$I_{t,x}(x) = \beta \left(\frac{b}{a} \right) \left[\frac{a}{2} \left[\left(1 \mp \frac{x}{c} \right) \right] \right]^3, \quad (3)$$

$$\beta \left(\frac{b}{a} \gg 1 \right) = \frac{1}{3}$$

where a is the height of the beam's cross section (Figure 1).

The equations above indicate that the solution to the problem (eq. 1) is heavily dependent on the joint geometry (eq. 3).

At this point, the predominant stress field in the adhesive (equivalent to the applied torsional moment) can be determined by imposing rotational equilibrium of an infinitesimal beam element belonging to the bond area:

$$\sigma_y(x,z) = -\frac{z}{I_x^*} \frac{dM(x)}{dx}, \quad (4)$$

where z is the transverse coordinate (Figure 1). Equation (3) demonstrates that the increase in torsional moment occurring at the ends of the infinitesimal element considered is balanced by the normal stresses that the adhesive exerts on the beam.

The corresponding predominant stress field ϵ_y (Figure 2) can be written taking into account the constitutive law as:

$$\epsilon_y(x,z) = \frac{\sigma_y(x,z)}{E_a^*} = -\frac{dM(x)}{dx} \frac{z}{E_a^* I_x^*}. \quad (5)$$

The compatibility equation permits to determine the joint's elastic strain, as relative rotation between the two beams' cross sections:

$$\Delta\theta(x) = \theta_2(x) - \theta_1(x) = -\frac{1}{K^*} \frac{dM(x)}{dx}. \quad (6)$$

Following a three dimensional finite element analysis, for non-tubular joints without tapered adherends, the mathematical approach was validated by comparing the predominant stress field given by equation (4) with that determined numerically, indicating an error on the stress peak of less than 4% [17].

The problem is bring back to determine section by section the torsional moment M solving the second order differential equation (1) in the case of tapered adherends (eq. (3)). The predominant stress and strain field in the adhesive and the joint's elastic strain can be obtained from equations (4), (5) and (6).

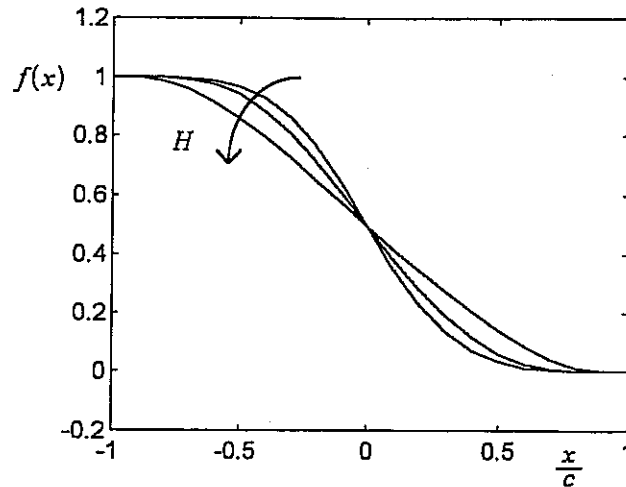


Fig. 3 Qualitative curve for $f(x)$ [torsional moments]

3 Closed form solution

The torsional moment $M(x)$ in the joint between the two beams can be written as:

$$\begin{aligned} M &= M_1(x) = M_t f(x) \\ M_2(x) &= M_t (1 - f(x)) \end{aligned} \quad (7)$$

since the sum of the moments absorbed by the two elements must be equivalent to the applied torsional moment M_t for each section. Function $f(x)$ has as its domain the real range $[-c, +c]$ and, in order for the boundary conditions for the torsional moments (eq. (1)) to be satisfied, must be unity at the extreme left and zero at the extreme right of the domain. Moreover, as the two beams must be symmetrical as regards torsional moment and stress, the following conditions must also obtain:

$$\begin{aligned} \left. \frac{df(x)}{dx} \right|_x &= \left. \frac{df(x)}{dx} \right|_{-x} \quad \forall x \\ 1 - f(x) &= f(-x) \end{aligned} \quad (8)$$

Introducing the adimensional coordinate $x^* = x/c$, the equation (1) can be rewritten as:

$$\begin{aligned} I_1(x^*) I_2(x^*) \frac{1}{c^2} \frac{d^2 M(x^*)}{dx^{*2}} + \\ + \frac{K^*}{G} (I_1(x^*) + I_2(x^*)) M(x^*) &= \quad (9) \\ &= -\frac{K^* M_t}{G} I_1(x^*) \end{aligned}$$

Considering thin adherends ($b/a \gg 1$) and putting the equations (3) and (7) in (9), we obtain the following differential equation:

$$\begin{aligned} H(1 - 3x^{*2} + 3x^{*4} - x^{*6}) \frac{d^2 f(x^*)}{dx^{*2}} + \\ - (2 + 6x^{*2}) f(x^*) &= - (1 - 3x^{*2} + 3x^{*4} - x^{*6}) \quad (10) \\ H &= \frac{Ga^3 b}{24K^* c^2} \end{aligned}$$

The solution of this differential equation must satisfy (8) and can be found in power series form:

$$f(x^*) = \frac{1}{2} + \sum_{n=1}^{\infty} l_{2n-1} x^{*2n-1} \quad (11)$$

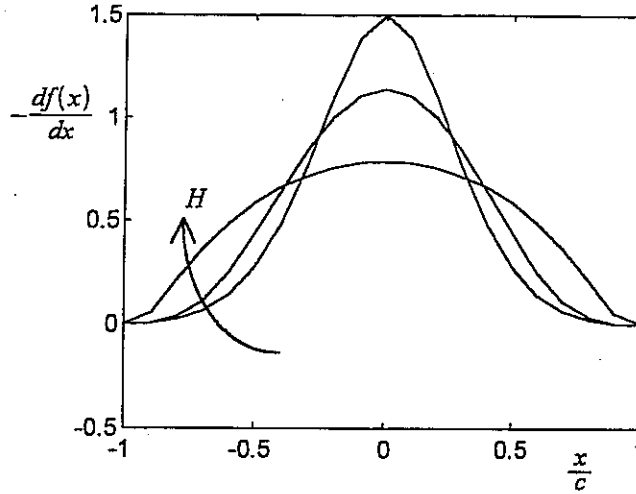


Fig. 4 Qualitative curve for $-\frac{df(x)}{dx}$ [relative rotations]

Through the principle of identity of polynomials, introducing this in (10) gives the following solution for the unknowns

$$l_{2n-1} = c_{2n-1} + d_{2n-1}l_1, \quad (c_1=0, d_1=1):$$

$$\begin{cases} c_3 = \frac{1}{2H} \\ d_3 = \frac{1}{3H} \end{cases}, \begin{cases} c_5 = \frac{10H+1}{20H^2} \\ d_5 = \frac{18H+1}{30H^2} \end{cases}$$

$$\begin{cases} c_7 = \frac{210H^2+70H+1}{420H^3} \\ d_7 = \frac{450H^2+78H+1}{630H^3} \end{cases} \quad (12)$$

$$(c,d)_{2n+1} = \frac{2}{H} + \frac{3(2n-1)(2n-2)}{(2n+1)(2n)} (c,d)_{2n-1} +$$

$$+ \frac{6}{H} - \frac{3(2n-3)(2n-4)}{(2n+1)(2n)} (c,d)_{2n-3} +$$

$$+ \frac{(2n-5)(2n-6)}{(2n+1)(2n)} (c,d)_{2n-5} \quad \forall n \geq 4$$

Once the coefficients l_i are known as a function of l_1 , the latter can be determined using the boundary condition $f(x^* = 1) = 0$:

$$l_1 = -\frac{\frac{1}{2} + \sum_{n=1}^{\infty} c_{2n-1}}{\sum_{n=1}^{\infty} d_{2n-1}} \quad (13)$$

The stress σ_y acting on the first beam at the bonded surface is found from (4):

$$\begin{aligned} \sigma_y(x,z) &= -\frac{M_1}{I_x^*} \frac{df(x)}{dx} z = \\ &= -\frac{M_1}{I_x^* c} z \sum_{n=1}^{\infty} (2n-1) l_{2n-1} \left(\frac{x}{c}\right)^{2n-2} \end{aligned} \quad (14)$$

Focusing attention on the plane $z=b/2$ (critical), the mean and maximum value of the stresses are:

$$\begin{aligned} \sigma_{y_{\text{med}}} &= \frac{1}{2c} \int_{-c}^{+c} \sigma_y(x) dx = \frac{M_1}{I_x^*} \frac{b}{4c} = \frac{3M_1}{b^2 c}, \\ \sigma_{y_{\text{max}}} &= \sigma_y(x=0) = -\frac{M_1}{I_x^*} \frac{b}{2c} l_1 \end{aligned} \quad (15)$$

Consequently, a stress concentration factor can be defined as:

$$\lambda = \frac{\sigma_{y_{\text{max}}}}{\sigma_{y_{\text{med}}}} = -2l_1 = \frac{1 + 2 \sum_{n=1}^{\infty} c_{2n-1}}{\sum_{n=1}^{\infty} d_{2n-1}} \quad (16)$$

The rotation expressions of the two beams are reduced to integrals of known functions:

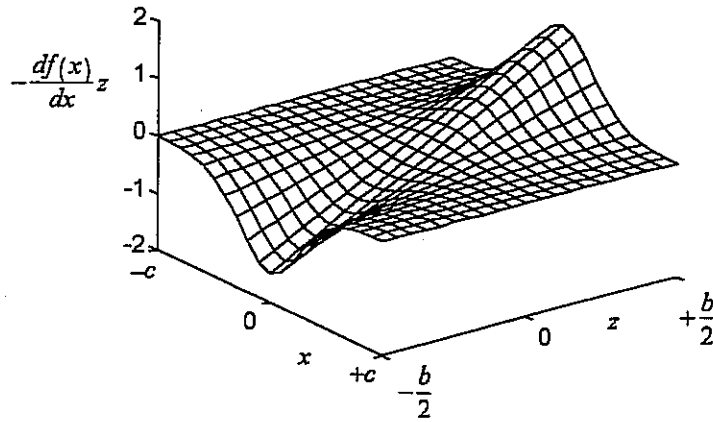


Fig. 5 Qualitative surface for $-\frac{df(x)}{dx} z$ [stresses and strains]

$$\theta_1(x) = \frac{M_t}{G} \int_{-c}^x \frac{f(t)}{I_1(t)} dt + \theta_1^0, \quad (17)$$

$$\theta_2(x) = \frac{M_t}{G} \int_{-c}^x \frac{(1-f(t))}{I_2(t)} dt + \theta_2^0$$

The compatibility equation (6) permits to determine the joint's elastic strain, as relative rotation. Fixing the reference system with $\theta_1^0 = 0$, the constant θ_2^0 is determined by inserting equations (17) into equation (6).

The results of the analysis described are presented in Figure 3,4,5. Figure 3 shows the curve for the function $f(x)$, governing torsional moment transmission in the joint, Figure 4 its derivative, which governs relative rotations and stresses in a constant z plane, and Figure 5 the stress field surface on the bond plane.

From equation (16) it is possible to obtain the value of the stress concentration factor. This value can be calculated in a approximated form as:

$$\lambda(H) \cong \frac{1 + 2 \sum_{n=1}^N c_{2n-1}(H)}{\sum_{n=1}^N d_{2n-1}(H)}, \quad (18)$$

where N is the finite number of terms considered. If N increases the series expansions converge and λ becomes N -independent.

Table 1 shows as λ (N -independent) changes with H .

4 Approximated solution

The H parameter for real joints assumes a value much smaller than 1 ($\approx 10^{-4}$). When H tends to zero the power series presented converges less rapidly and it is possible to have some numerical problems. In this case an approximated solution can be used. If we set $H=0$ in (10), the order of this differential equation becomes zero and the function $f(x)$ can be directly obtained. By applying equation (3), $f(x)$ assumes the physical meaning of relative torsional rigidity and coefficient of distribution:

$$f(x) = \frac{I_1(x)}{I_1(x) + I_2(x)}. \quad (19)$$

As expected, this indicates that the stress field is extremely sensitive to external geometry. The simplified solution (19) satisfies the boundary conditions of the problem and the symmetrical conditions (8).

The correspondent torsional moment becomes:

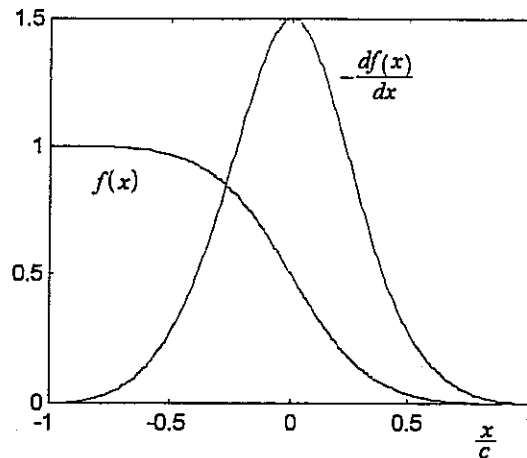


Fig. 6 Curves for $f(x)$ and its derivative ($H \rightarrow 0$)

$$M_1(x) = M, -M_2(x) = \frac{1 - 3\left(\frac{x}{c}\right) + 3\left(\frac{x}{c}\right)^2 - \left(\frac{x}{c}\right)^3}{2 + 6\left(\frac{x}{c}\right)^2} M, \quad (20)$$

The stress and strain predominant field become as follows:

$$\sigma_y(x, z) = \frac{(1 - \nu_a) E_a}{(1 + \nu_a)(1 - 2\nu_a)} \varepsilon_y(x, z) = \frac{18M_1}{cb^3} \left(\frac{\left(\frac{x}{c}\right)^2 - 1}{1 + 3\left(\frac{x}{c}\right)^2} \right) z, \quad \lambda = \frac{\sigma_{y_{max}}}{\sigma_{y_{med}}} = 3, \quad (21)$$

and the relative rotation between the two beams is:

$$\Delta\theta(x) = \theta_2(x) - \theta_1(x) = \frac{18(1 + \nu_a)(1 - 2\nu_a)hM_1}{(1 - \nu_a)E_a b^3} \left(\frac{\left(\frac{x}{c}\right)^2 - 1}{1 + 3\left(\frac{x}{c}\right)^2} \right). \quad (22)$$

The torsional moment absorbed by the two beams (20) is proportional to the correspondent torsional stiffness (which in turn is proportional to the cube of the height).

In any given section of the overlap, the top beam will thus tend to absorb almost all of the transmitted torsional moment, whose maximum variation will consequently take place at the centerline of the joint. The variation in torsional moment is balanced by the stresses (21) that the adhesive transmits to the beam. By contrast in the situation without tapered adherends joints (Pugno and Surace, 2000), these stresses will thus also be highest at the centerline. The stress concentration factor expressed is equal to 3. It is important to observe that it is an high upper bound for every practical value of H (Table 1). This stress concentration factor value is the same as we find in a linear elastic infinite plate with a circular hole subject to tension.

Figure 6 shows the function (19) and its derivative (torsional moment and stress/strain field in a $z = \text{const.}$ plane or relative rotation).

Clearly this approximated solution cannot be at the same time statically (equilibrium) and kinematically (compatibility) determined: indeed the difference between equations (17), inserting eq. (19), is a constant value in disagreement with equation (22). In order to satisfy both equilibrium and compatibility equations the exact solution has to be considered.

$H =$	m	-6	-5	-4	-3	-2	-1	0	1	2	3	4
10^m	λ	3	2.999	2.997	2.977	2.824	2.279	1.567	1.163	1.033	1.004	1

Table 1 Stress concentration factor varying $H = 10^m$ (real joint: m around -4)

5 Conclusions

A closed form solution for the problem of a non-tubular bonded joint with tapered adherends in torsion has been presented. The torsional moment transmission along the overlap, the predominant stress and strain fields in the adhesive and the joint's compliance have been obtained in series expansions. An approximated solution has been also presented.

It has been shown that, by contrast with the situation for conventional non-tubular joints, the stresses for tapered adherends will be surprisingly highest not at the ends of the adhesive layer but at its centerline. Finally, the correspondent stress concentration factor has been evaluated via the exact solution. It appears substantially constant and close to three.

Acknowledgements

The author would like to thank his researcher supervisors Prof. A. Carpinteri and the Italian National Research Council (CNR) for funding the work described in this paper.

References

- [1] Adams, R. D. and Peppiatt, N. A. Stress analysis of adhesive bonded tubular lap joints. *Journal of Adhesion* 9, pp. 1-18, 1977.
- [2] Alwar, R. S. and Nagaraja, Y. R. Viscoelastic analysis of an adhesive tubular joint. *Journal of Adhesion*, Vol. 8, pp. 79-92, 1976.
- [3] Carpinteri, A. *Structural Mechanics-A Unified Approach*. E & FN Spon, 1999.
- [4] Chen, D. and Cheng, S. Torsional stress in tubular lap joints. *International Journal of Solids and Structures*, Vol. 29, pp. 845-853, 1992.
- [5] Chen, D. and Cheng, S. Torsional stresses in tubular lap joints with tapered adherends. *Journal of Engineering Mechanics-ASCE*, Vol. 118, pp. 1962-1973, 1992.
- [6] Chon, C. T. Analysis of tubular lap joint in torsion. *Journal of Composite Materials*, Vol. 16, pp. 268-284, 1982.
- [7] Goland, M. and Reissner, E. The stresses in cemented joints. *Journal of Applied Mechanics*, Vol. 11, pp. 17-27, 1944.
- [8] Graves, S. R. and Adams, D. F. Analysis of a bonded joint in a composite tube subjected to torsion. *Journal of Composite Materials*, Vol. 15, pp. 211-224, 1981.
- [9] Hipol, P. J. Analysis and optimization of a tubular lap joint subjected to torsion. *Journal of Composite Materials*, Vol. 18, pp. 298-311, 1984.
- [10] Lee, S. J. and Lee, D. G. An iterative solution for the torque transmission capability of adhesively-bonded tubular single lap joints with non-linear shear properties. *Journal of Adhesion*, Vol. 53, pp. 217-227, 1995.
- [11] Lee, S. W., Lee, D. G. and Jeong K. S. Static and dynamic torque characteristics of composite cocured single lap joint. *Journal of Composite Materials*, Vol. 31, pp. 2188-2201, 1997.
- [12] Lubkin, J. L. and Reissner, E. Stress distribution and design data for adhesive lap joints between circular tubes. *Transaction of ASME*, Vol. 78, pp. 1213-1221, 1956.
- [13] Matsui K. Size effects on nominal ultimate shear stresses of adhesive-bonded circular or rectangular joints under torsion. *International Journal of Adhesion and Adhesives*, Vol. 11, pp. 59-64, 1991.
- [14] Medri, G. Viscoelastic analysis of adhesive bonded lap joints between tubes under torsion. *Journal of vibration acoustics stress and reliability in design-transactions of the ASME*, Vol. 110, pp. 384-388, 1988.
- [15] Pugno, N. *Non tubular bonded joints under torsion*. Philosophy Doctorate Thesis, Department of Structural Engineering, Politecnico di Torino, Torino, Italy, 1998.
- [16] Pugno, N. Optimising a non-tubular adhesive bonded joint for uniform torsional strength. *International Journal of Materials and Product Technology*, Vol. 14, 476-487, 1999.
- [17] Pugno, N. and Surace, G. Non-tubular bonded joint under torsion: Theory and numerical validation. *Structural Engineering and Mechanics*, Vol. 10, No. 2, pp. 125-138, 2000.
- [18] Pugno, N. and Surace G. Tubular bonded joint under torsion: analysis and optimization for uniform torsional strength. *Journal of Strain Analysis for Engineering Design*, Vol. 1, pp. 17-24, 2001.

- [19] Rao, M. D. and Zhou, H. Vibration and damping of a bonded tubular lap joint. *Journal of Sound and Vibration*, Vol. 178, pp. 577-590, 1994.
- [20] Reedy, E. D. and Guess, T. R. Composite-to-metal tubular lap joints strength and fatigue resistance. *International Journal of Fracture*, Vol. 63, pp. 351-367, 1993.
- [21] Vonesebeck, G., Kising, M. and Neuhof, U. Investigation on ceramic-metal joints for shaft-hub connections in gas-turbines. *Journal of engineering for gas turbines and power-transactions of the ASME*, Vol. 118, pp. 626-631, 1996.
- [22] Zhou, H. M. and Rao, M. D. Viscoelastic analysis of bonded tubular joints under torsion. *International Journal of Solids and Structures*, Vol. 30, pp. 2199-2211, 1993.